horticulturae

MDPI

Article

Transcriptional Insights into Lily Stem Bulblet Formation: Hormonal Regulation, Sugar Metabolism, and Transcriptional Networks in LA Lily 'Aladdin'

Kewen Zhang [1,†], Tong Lyu [2,†] and Yingmin Lyu [1,*]

[1] Beijing Key Laboratory of Ornamental Plants Germplasm Innovation & Molecular Breeding, China National Engineering Research Center for Floriculture, College of Landscape Architecture, Beijing Forestry University, Beijing 100083, China
[2] Beijing Flower Engineering Technology Research Center, Plant Institute, China Botanical Garden North Garden, Beijing 100093, China
* Correspondence: luyingmin@bjfu.edu.cn
† These authors contributed equally to this work.

Abstract: Bulblets, as the main reproductive organ of lilies, have a tremendous impact on the reproductive efficiency of lilies. Cytokinin is known to promote the formation of lily bulblets, but little is known about the mechanisms involved. In this study, a combination of full-length transcriptome and high-throughput RNA sequencing (RNA-Seq) was performed at the leaf axils of LA lily 'Aladdin' to characterize the transcriptional response to 6-BA treatment during the critical period of stem-to-bulblet transition. Kyoto Encyclopedia of Genes and Genomes (KEGG) analysis showed that 6-BA treatment caused significant changes in starch and sucrose metabolism and plant hormone balance. In particular, the high expression of *SUS1* and *TPS6* in the 6-BA-treated group suggests that sucrose may act as a key signal to promote bulblet initiation. Furthermore, the induction of elevated expression of genes associated with cytokinin and auxin transport and signaling is crucial for initiating bulblet emergence and stimulating growth. WGCNA analysis revealed that hub TFs such as BLHs, ARFs, HD-ZIPs, AP2/ERFs, and SBPs were significantly overexpressed with genes involved in carbohydrate metabolism and phytohormone signaling, which warranted more in-depth functional studies. This study enriches the understanding of plant hormone-related genes, sugar metabolism-related genes and various transcription factors in the regulation of plant organ development, and lays the foundation for further studies on the molecular mechanisms of lily stem bulblet formation.

Keywords: LA hybrid lily; stem bulblet formation; 6-benzylaminopurine (6-BA); phytohormone biosynthesis and signaling; starch and sucrose metabolism

Citation: Zhang, K.; Lyu, T.; Lyu, Y. Transcriptional Insights into Lily Stem Bulblet Formation: Hormonal Regulation, Sugar Metabolism, and Transcriptional Networks in LA Lily 'Aladdin'. *Horticulturae* **2024**, *10*, 171. https://doi.org/10.3390/horticulturae10020171

Academic Editors: Margherita Beruto, Emmy Dhooghe and Bruce Dunn

Received: 15 December 2023
Revised: 4 February 2024
Accepted: 11 February 2024
Published: 14 February 2024

1. Introduction

Lily (*Lilium* spp.), an old worldwide flower, has high ornamental and edible value. Bulblets are the reproductive organ of lilies, and the quantity and quality of bulblets have a great influence on the yield of lilies. Previous studies mainly focused on the formation of lily bulbs under in vitro conditions, and very few studies have been carried out on their natural proliferation, especially in the absence of a clear molecular regulatory mechanism [1]. LA hybrid lily 'Aladdin' has a very strong self-propagation ability under natural conditions, and can spontaneously form a large number of good quality underground-stem bulblets on underground stems, which is an excellent test material to study the mechanism of lily bulb formation under natural conditions [2,3].

The synthesis and signaling of several plant hormones have been reported in the literature to act on the formation of bulblets, like auxin (AUX), cytokinin (CK), ethylene (ETH), gibberellin (GA), abscisic acid (ABA), etc. [4–6]. Among them, cytokinin and auxin

are considered to be important hormones regulating bulb formation in plants [7,8]. Previous studies found that applying exogenous cytokinin (6-BA) to LA hybrid lily 'Aladdin' can accelerate the speed of underground stem-bulblet initiation and increase the number of bulblet occurrence [9]. In *Lilium lancifolium*, 6-BA promotes bulbil initiation while lovastatin delays it, and genes involved in cytokinin metabolism and signaling undergo opposite changes [10]. According to previous studies, auxin may have a dual role in lily bulb organ formation, with auxin acting as a promoter during the initiation phase of organ induction but inhibiting the response to auxin at a later stage to maintain proper hormonal homeostasis within the newly formed meristematic tissue [11–13]. The exogenous application of IAA promotes the formation of bulbils, but the inhibitors of auxin transport, NPA, TIBA, and the inhibitor of auxin function, PCIB, inhibited the formation of bulbils in in vitro stem segments of *Lilium lancifolium* to different extents [14]. In addition, it was found that the application of IAA induces aerial bulbils on the cut surface of the upper stem through a process similar to callus formation [15]. In a recent study, 2,4-dichlorophenoxyacetic acid (2,4-D) significantly increased the regeneration rate of in vitro bulblets in *L. brownii* and *L. brownii* var. giganteum [16].

Recent studies showed that carbohydrate metabolism was also associated with bulb formation [17,18]. In *Lilium davidii* var. unicolor, genes involved in starch synthesis (ADPG pyrophosphorylase gene *AGP*, starch branching enzyme gene *SBE*, soluble starch synthase gene *SSS,* and bound starch synthase gene *GBSS*) were mainly highly expressed at the emergence of small bulbs and during later bulb development; therefore, it is speculated that starch may play a key role in later bulb development [18]. A previous study demonstrated that bulbing involves a shoot-to-bulblet transition and the higher expression of the sucrose synthase gene (*LohSuSy*) could accelerate this transformation process [19]. In *Lycoris sprengeri*, a study indicated a sugar-mediated model of the regulation of vegetative propagation in which high cell wall invertase (*CWIN*) expression or activity could promote bulblet initiation via enhancing apoplasmic unloading of sucrose or sugar signals [20].

Stem bulblets, formed in the leaf axils of the above- and below-ground stems of lilies, are axillary organs and originate from axillary meristematic tissue (AM) [2,21]. In *Arabidopsis thaliana*, numerous studies have revealed that several transcription factors affect AM initiation [22,23]. However, regarding the molecular regulation of bulblet formation, only a small number of genes have been validated so far, and their regulatory mechanisms are still unclear. It was demonstrated that HOMEOBOX PROTEIN KNOTTED-1-LIKE (LaKNOX1) interacts with LaKNOX2 and BEL1-LIKE HOMEBOX (LaBEL1) to simultaneously regulate multiple plant hormones to achieve proper hormone homeostasis, thereby exerting a positive effect in stem bulblet formation in *L.* 'Aladdin' [9]. In *Agave tequilana*, *AtqKNOX1* and *AtqKNOX2* genes were induced at bulbil initiation and their expression increased with bulbil development [24]. In *Lilium lancifolium*, the *Argonaute 1* (*LlAGO1)* was suggested to play an positive role in the formation of bulbils [25]. In other studies, the *LoAGO1* gene was also found to play a role in meristem induction along with other genes regulating growth hormone signaling such as *TOPLESS* (*LoTPL*) and *AUXIN SIGNALING F-BOX 3* (*LoAFB3*) [4]. According to a previous study, cytokinin type-B response regulators *LlRRs* could bind to the promoters of *LlWOX9* and *LlWOX11* and encourage their transcription to promote bulbil generation [26]. In addition to TFs associated with AM initiation, TFs associated with organ boundaries were also shown to affect bulb production. In the oriental lily 'Siberia', a *LoLOB18* gene belonging to the LOB (lateral organ boundaries domain) transcription factor family was demonstrated to have a positive regulatory role in bulb formation by VIGS experiments [27].

In this study, we applied 6-BA to the underground stems of lilies, 40 days after planting, and analyzed RNA sequences of treated and control samples on days 1, 10, and 20 thereafter. We investigated the patterns of gene expression changes during lily bulb development related to starch and sucrose metabolism, hormone synthesis and signaling, and some transcription factors related to axillary bud initiation, and then constructed the network relationships of these genes by WGCNA analysis. In conclusion, our results provide insight

into the molecular regulatory mechanisms regulating lily bulblet formation, which will contribute to future studies to improve the reproductive efficiency of lily plants.

2. Materials and Methods

2.1. Plant Materials

At Beijing Forestry University (BJFU) (116.3E, 40.0N), the study was carried out in the identical climate-controlled facility. Three-year-old LA (*Lilium longiflorum* × *Lilium asiatic*) hybrid cultivars 'Aladdin' with similar diameters were selected as experimental materials. The planted lilies were divided into two groups, and 100 mg/L of 6-BA (total 25 mg) and water (as control) were applied to the underground stems 40 days after planting. The second application was repeated after 48 h. We collected leaf axils of underground stems at 1, 10, 20, and 25 days after application, as with the control group. The leaf axils (including leaf axil tissues and part of the stem bode) were cut with a double-sided razor blade at about 0.2 mm thickness. Samples of each period and group were mixed from three lily samples, each containing 3–5 leaf axils, and three biological replicates were performed. The control samples were named C1, C10, C20, and C25 while the 6-BA treated groups were named B1, B10, B20, and B25. The collected leaf axil samples were wrapped in tin foil bags and quickly frozen in liquid nitrogen for 30 min, and then transferred to a −80 °C refrigerator for storage until further use.

2.2. Morphological and Histological Observation

Morphological changes of bulblet initiation in *L.* 'Aladdin' were observed under a stereomicroscope (SP8 SR, Lecia, Wetzlar, Germany). The induction rate of bulblets was calculated as follows: induction rate = number of axils that produced axillary meristems/total number of underground axils. Samples from leaf axils with partial leaves were fixed with FAA (70% ethanol: glacial acetic acid: formalin, 90:5:5) at 4 °C for 24 h. Fixed samples were dehydrated and embedded in paraffin wax through an ethanol gradient, and longitudinal sections were prepared using a sectioning machine (Leica HistoCore BIOCUT, Wetzlar, Germany). The resulting sections were stained with safranin–alcian green, and the morphological and structural characteristics of the samples were subsequently observed under a light microscope and recorded.

2.3. RNA Extraction and Quality Assessment

Total RNA was extracted using a Plant RNA Extraction Kit (RN53, Aidlab, Beijing, China) according to the manufacturer's instructions, and treated with RNase-free DNase I to remove residual DNA contamination. The integrity and purity of the total RNA were determined using a NanoDrop-1000 UV spectrophotometer (Thermo Fisher Scientific, Waltham, MA, USA) and 1.2% agarose gel electrophoresis.

2.4. PacBio Iso-Seq Library Preparation, Sequencing, and Analysis

Total RNA from above-ground stem axils of C1, C10, C20, B1, B10, and B20 were mixed in equal amounts and sequencing libraries were constructed through the PacBio platform to obtain the full-length transcriptome sequences of *L.* 'Aladdin'. First, Clontech SMARTer PCR cDNA Synthesis Kit was used to reverse translate total RNA to first-strand cDNA, and then PCR amplification was performed to synthesize double-strand cDNA. Second, SMRTbell library construction was performed after the purification of the products. Finally, the SMRTbell library was annealed with primers and polymerase and sequenced using MagBead Loading.

The raw reads were analyzed, and circular consensus sequence (CCS) sequences were extracted using SMRT Link v6.0 [28]. The primers, barcodes, poly(A) tails, and tandems were then removed to obtain full-length non-chimeric sequences (FlNC). Subsequently, the full-length non-chimeric (FLNC) reads were clustered by error-corrected iterative clustering (ICE) to generate clustered consensus heterodimers. Next, low quality isomers were further corrected by the LoRDEC tool [29] using Illumina short reads obtained from the same

lily-leaf axil samples. CD-HIT-v4.6.7 software was used to remove redundant sequences using a threshold of 0.99 identity to obtain the final transcriptome isoform sequence.

2.5. Illumina Transcriptome Library Preparation, Sequencing, and Analysis

To characterize the expression of transcriptomic differential gene sets during *L.* 'Aladdin' stem bulblet initiation, total RNA from aboveground stem axils of C1, C10, C20, B1, B10, and B20 was extracted for RNA-Seq with two replications for each sample. First, after the RNA test was passed, the mRNA with poly(A) structure was enriched. Then the mRNA was broken into short fragments, and the RNA was used as a template to synthesize double-stranded cDNA and purified. The purified double-stranded cDNA was then subjected to end repair, Then, the purified double-stranded cDNA was end-repaired, sequencing junction and A-tail structure were added, fragment size was selected, with PCR amplification and purification of PCR products. The final PCR products were sequenced using Illumina HiSeqTM 2000 (Illumina, San Diego, CA, USA).

Using in-house Perl scripts with default parameters, we filtered the raw data (raw reads) generated from the Illumina sequencing platform, including reads containing adapters, reads containing more than 10% unknown nucleotides (N), and low-quality reads containing more than 50% low-quality (Q-value $\leq$ 10) bases. The rRNA removed high-quality clean reads were mapped to the reference transcriptome using the short reads alignment tool Bowtie2 [30] by default parameters. These clean reads were then mapped to the full-length transcriptome sequences of *L.* 'Aladdin' obtained by PacBio Iso-Seq using HISAT2 [31].

2.6. Functional Annotation of Tanscripts, Identification of Differentially Expressed Genes (DEGs), and Functional Enrichment

We performed BLASTx searches of all the identified transcripts against seven public databases, including the NR, NT, Pfam, KOG, Swiss-Prot, KEGG, and GO databases, with a threshold E-value of $\leq 10^{-5}$. Gene expression levels were calculated as fragments per kilobase of transcript per million mapped reads (FPKM) [32]. DESeq2 was utilized to conduct a differential expression study between two groups. Based on the Benjamini and Hochberg method, differential expression was defined as a fold change of more than 1 with an adjusted e-value (false discovery rate, FDR) of less than 0.05.

2.7. Identification of Co-Expression Network Modules

Gene co-expression modules were created using the weighted gene co-expression network analysis program for R (WGCNA, version 1.47) [33]. To construct co-expression modules, the WGCNA package used the block-wise module construction feature with detailed settings to import the transcript expression values. This TOMType was unsigned, the mergeCutHeight was 0.8, and the minModuleSize was 50. The networks were visualized using Cytoscape v3.9.1 [34].

2.8. Quantitative Real-Time PCR Validation

To validate the RNA-Seq data, 12 significant DEGs involved in the plant hormone signal transduction pathway, starch and sucrose metabolism, and transcription factors were selected randomly, and qRT–PCR assays were performed. cDNA was synthesized from total RNA using Prime Script II 1st strand cDNA Synthesis Kit (Takara, Shiga, Japan). According to the manufacturer's protocol, the cDNA template was fully mixed with SYBR R® qPCR mix (Takara, Japan) and used for qRT–PCR in a Bio-Rad/CFX ConnectTM Real-Time PCR Detection System (Bio-Rad, Irvine, CA, USA). Gene expression levels were analyzed with the $2^{-\Delta\Delta CT}$ method [35] using the *TIP41* gene of *Lilium* [36] as internal standards. All analytical procedures were repeated on three biological replicates. Specific quantitative primers were designed using NCBI Primer-BLAST (http://www.ncbi.nlm.nih.gov) (accessed on 12 July 2022) (Table S1).

3. Results

3.1. Morphological and Histological Observations on Bulblet Formation after Application of 6-BA

To understand the formation of stem bulblet initiation in *L.* 'Aladdin', samples were collected from underground leaf axils at 1d, 10d, 20d, and 25d after 6-BA was applied to observe it morphologically and histologically (Figure 1). Based on our observations, there were no apparent changes in the axillary region of the leaves (Figure 1a,e) one day after treatment with 6-BA (B1). Through paraffin section imaging, in comparison to the B1 stage, cells in the axils at the B10 stage exhibited a more closely arranged pattern, with increased cell numbers, and more prominent cell nuclei (Figure 1e,f). At the B20 stage, the distinct band-like protrusions in the axillary region became clearly visible (Figure 1c), and the dense cells had formed axillary meristematic tissue (Figure 1g). By the B25 stage, these structures developed into bulbous formations (Figure 1d), with the axils distinctly showing the initiation of bulblet primordia, including axillary meristems and scale primordia (Figure 1h). Thus, we classified the process facilitated by 6-BA into the axillary meristem activation stage (B1–B10), bulblet initiation stage (axillary meristem formation stage) (B20), and bulblet primordia formation stage (B25). In contrast, morphological and histological observations in the control group treated with distilled water during the corresponding time periods did not reveal the formation of bulbs (Figure S1). During the bulblet initiation stage (B20), we observed the formation of axillary meristems in both the control and treatment groups. The results revealed a significantly higher induction rate in the 6-BA treatment group compared to the control group ($p < 0.0001$), with no axillary bud formation observed in the control group (Figure S2). Therefore, we hypothesize that the use of 6-BA plays a very important role in the germination of underground stem bulblets.

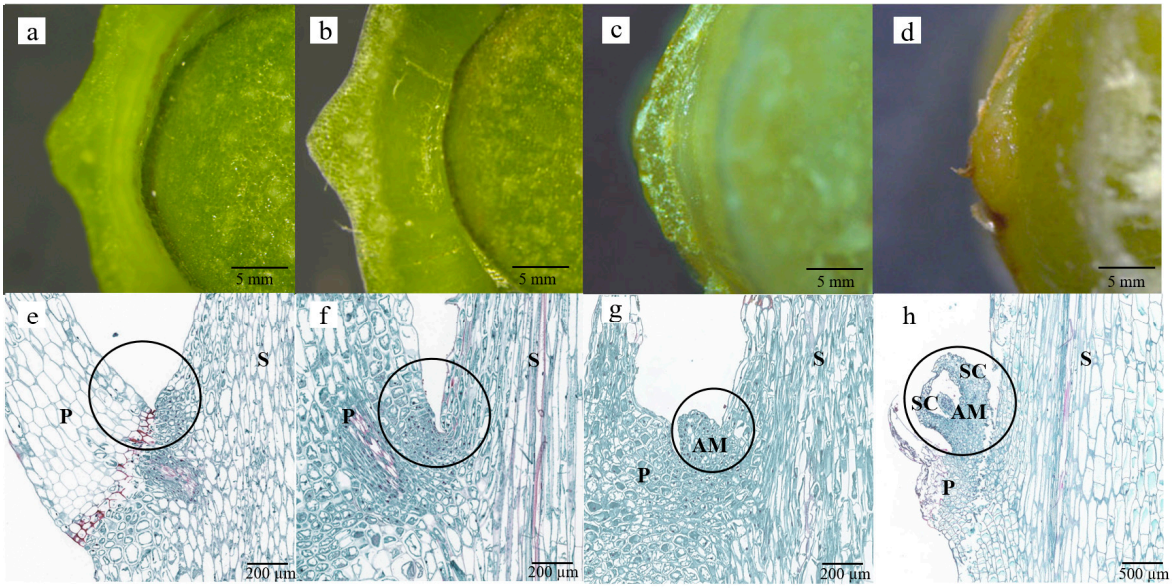

Figure 1. Morphology and anatomy of stem bulblet formation under the influence of 6-BA. Scale bar for sample images (**a**–**d**) = 5 mm; scale bar for microscope images (**e**–**g**) = 200 and (**h**) = 500 μm. P, Petiole; S, stem; SC, scale; AM, axillary meristem; black circle, leaf axil.

3.2. RNA-Seq Analysis of L. 'Aladdin'

For the purpose of obtaining a comprehensive annotation of the genes of *L.* 'Aladdin', a total of 32,400 full-length non-redundant transcripts were obtained using PacBio SMRT sequencing. The transcript sequences ranged from 54 to 7596 base pairs (bp) in length, with an average transcript length of 1362.86 bp and an N50 of 1783 bp (Figure S3a). Of the clean reads obtained from Illumina RNA-Seq, 80.33% was mapped to the reference transcripts (Table S2), and the number of transcripts annotated in the four major protein databases, Nr,

SwissProt, KEGG and KOG, was 29,244, 16,404, 18,679, and 25,547, respectively. Additionally, out of the 32,400 transcripts, 12,975 were annotated in all four major databases, while 3011 transcripts were not annotated (Figure S3b).

The differentially expressed genes (DEGs) were determined by the *L.* 'Aladdin' 6-BA treated and control groups at three stages (1d, 10d, 20d). We screened for expression levels $|\log2(FC)| > 1$ and FDR < 0.05 as DEGs by comparing each comparison group. First, three comparison groups were obtained by comparing samples from different treatments during the same time period. In total, 2275, 4704, and 4378 of the DEGs were differentially expressed between B1 versus (vs.) C1, B10 vs. C10, and B20 vs. C20, respectively. Meanwhile, 755, 2196, and 1999 DEGs were specific for B1 vs. C1, B10 vs. C10, and B20 vs. C20, respectively (Figure S3e). Among the three comparison groups, B10 vs. C10 had the highest number of DEGs with 4704, including 2519 up-regulated genes and 2185 down-regulated genes. This was followed by B20 vs. C20 with 4378 DEGs, including 2614 up-regulated and 1764 down-regulated genes. The least number of differential genes was in the B1 vs. C1 comparison group with only 2275, including 1393 up-regulated and 882 down-regulated genes (Figure S3c). Meanwhile, we compared samples at different time points after the application of 6-BA and obtained three comparison groups: B10 vs. B1, B20 vs. B1, and B20 vs. B10. Among these three comparison groups, the highest number of commonly expressed DEGs was observed, totaling 2505 (Figure S3f). Additionally, all three comparison groups showed a higher number of upregulated genes than downregulated genes, and the number of upregulated DEGs increased with the number of days of application (Figure S3d).

To validate the reliability of the RNA-Seq data, 12 DEGs were selected for qRT–PCR analysis. We found that the RNA-seq and RT-qPCR data were similar and yielded consistent expression patterns. Therefore, the experimental results confirmed the accuracy and reliability of the sequencing results (Figure S4).

3.3. KEGG Pathway Enrichment Analysis of DEGs

We performed KEGG pathway enrichment analysis for DEGs obtained from B1 vs. C1, B10 vs. C10, B20 vs. C20, B10 vs. B1, B20 vs. B1, and B20 vs. B10 comparisons, respectively (Figure 2). There was a significant difference in KEGG enrichment between B1 and C1 DEGs, with "plant hormone signal transduction" the most significant, followed by "biosynthesis of secondary metabolites", "biosynthesis of amino acids", "plant circadian rhythm", "linoleic acid metabolism", and "carbon metabolism" (Figure 2a). For B10 vs. C10, DEGs were mainly enriched in "biosynthesis of secondary metabolites", "carbon fixation in photosynthetic organisms", "metabolic pathways", "starch and sucrose metabolism", and "plant hormone signal transduction pathway" (Figure 2b). Additionally, the DEGs for B20 vs. C20 were mainly enriched in the "biosynthesis of secondary metabolites", "starch and sucrose metabolism", "glyoxylate and dicarboxylate metabolism", "garbon metabolism", "metabolic pathways" and "plant hormone signal transduction" (Figure 2c). In the comparison of B10 vs. B1, DEGs were significantly enriched in the pathways of "plant hormone signal transduction", "plant-pathogen interaction", "biosynthesis of secondary metabolites", and "MAPK signaling pathway-plant" (Figure 2d). Similar to B10 vs. B1, the two most significantly enriched pathways for DEGs in the B10 vs. B1 comparison were "plant hormone signal transduction" and "plant-pathogen interaction". Additionally, DEGs were also enriched in the "starch and sucrose metabolism" pathway (Figure 2e). Furthermore, in the comparison B20 vs. B10, DEGs were significantly enriched in the pathways of "plant hormone signal transduction" and "starch and sucrose metabolism" (Figure 2f). In all six comparative groups, DEGs were enriched in the pathway of "plant hormone signal transduction". In addition, except for the two comparative groups B1 vs. C1 and B10 vs. B1, all other comparative groups were enriched in the pathway of "starch and sucrose metabolism". These results suggest that 6-BA promotes phytohormone responses throughout bulblet emergence and promotes bulblet formation through signal transduction. Moreover, starch and sucrose metabolism as well as sugar signaling may play an important role in the bulblet process.

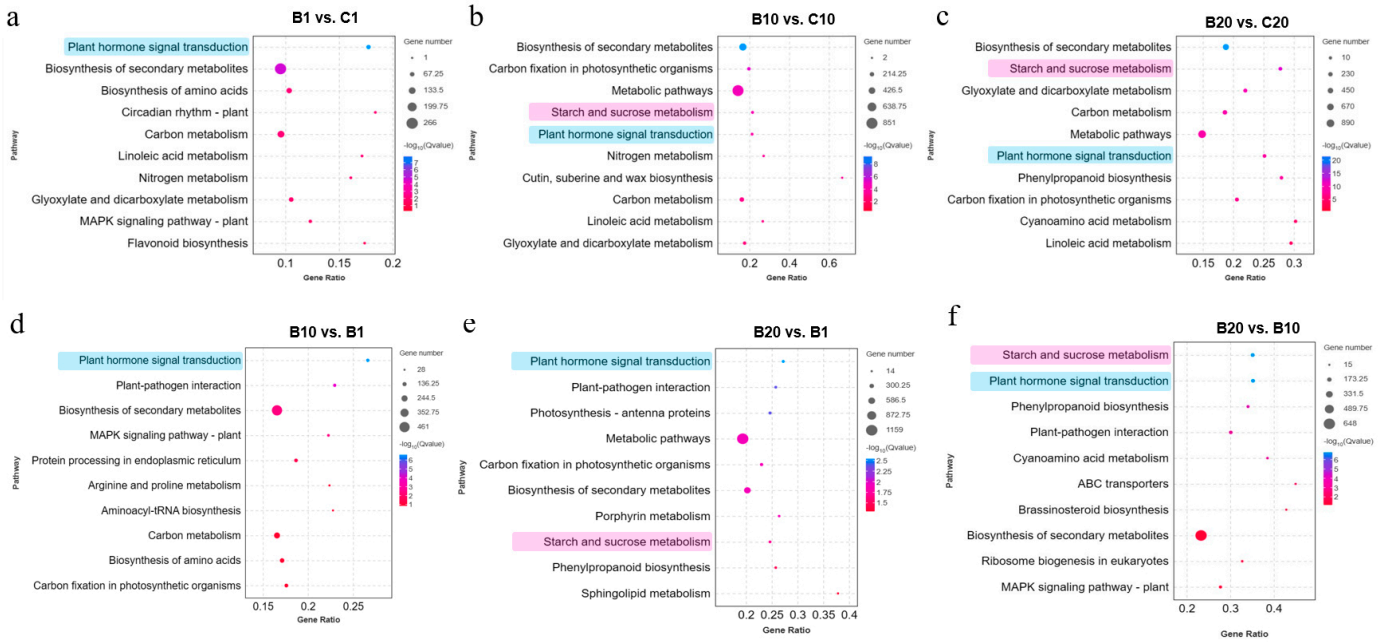

Figure 2. KEGG enrichment analyses of stem bulblet initiation. The top 10 KEGG pathways of the DEGs in each comparison: (**a**) B1 vs. C1, (**b**) B10 vs. C1, (**c**) B20 vs. C20, (**d**) B10 vs. B1, (**e**) B20 vs. B1, (**f**) B20 vs. B10. The phytohormone signaling pathway is highlighted in blue, while the starch and sucrose pathway is highlighted in red.

3.4. Expression of Genes Involved in Starch and Sucrose Metabolism Pathways under 6-BA Treatment

In our research, according to the KEGG enrichment, the 6-BA treatment induced genes related to starch and sucrose metabolism. Therefore, we discovered 25 genes associated with this pathway that showed differences in expression in at least one comparison (Figure 3). Seven *SUS1* genes encoding sucrose synthases were upregulated at B10 compared to C10. Compared to the control group, seven genes encoding sucrose synthases (*SUSs*) in the 6-BA-treated group were upregulated at different time points. Among them, two *SUS1* genes (Isoform0001718 and Isoform0028472) exhibited an upregulation pattern in the B10 vs. C10 comparison, with *SUS1* (Isoform0001718) showing a particularly remarkable upregulation fold change of 14.60 (Table S3). Sucrose may be a signal that promotes bulb growth by upregulating genes in the T6P pathway. In our data, the gene *TPS* regarding trehalose-phosphate synthase and the gene *TPP* regarding trehalose-phosphate phosphatase presented distinct expression patterns in the 6-BA treatment and control groups, respectively. Among them, a higher level of expression was observed in B20 than in C20 for seven *TPS* isoforms. However, another two *TPP* transcripts (*TPPG* and *TPP6*) exhibited an opposite expression profile by the 6-BA treatment. Particularly, 6-BA consistently decreased *TPP6* expression in all three periods. Genes encoding sucrose phosphate synthase, including *SPS2* (Isoform0009502) and S*PS4* (Isoform0009583), were up-regulated in the B20 vs. C20 comparison. In addition, *INV* genes (Isoform0004628 and Isoform0031226), which are related to fructose and glucose synthesis, showed an up-regulated expression pattern after 10 d and 20 d of 6-BA application compared to the control group. One *AMY*3 gene encoding alpha-amylase, which degrades starch to glucose, is highly expressed at B10. Moreover, *PGMP* (phosphoglucomutase) and *AGPS*1 (ADP-glucose pyrophosphorylase catalytic subunit) genes related to glucose metabolism were upregulated at B10. Additionally, one *AGPS1* (Isoform0030445) was also expressed upregulated at B20.

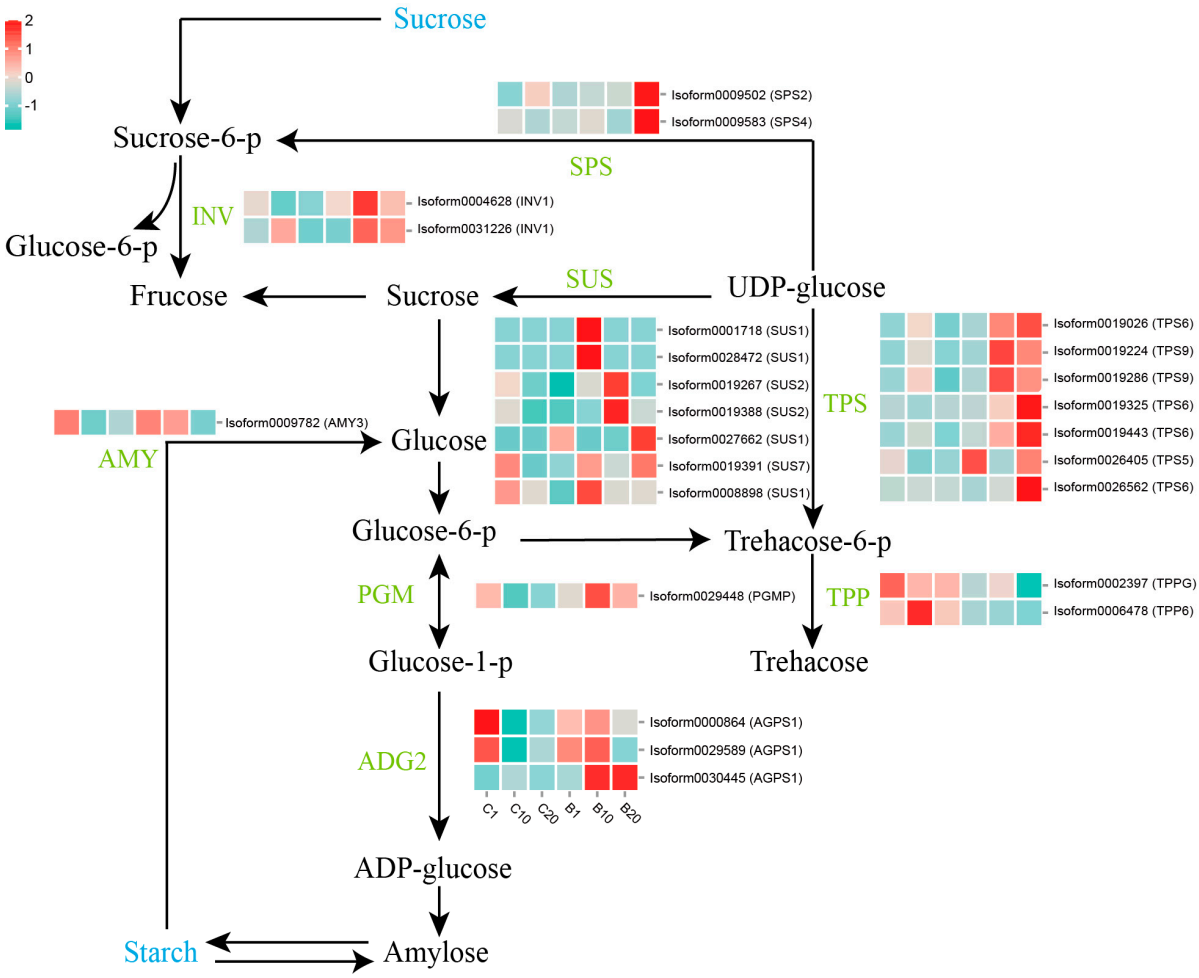

Figure 3. Expression of DEGs related to starch and sucrose metabolism pathways in 6-BA treated and control groups. The gene expression levels are standardized into Z−scores, with red indicating upregulation and purple indicating downregulation.

3.5. Analysis of DEGs Involved in Phytohormone Biosynthesis and Signal Transduction Pathway during Stem Bulblet Initiation

Studies have shown that plant hormones such as auxin (AUX), cytokinin (CK), abscisic acid (ABA), gibberellin (GA), brassinosteroid (BR), ethylene (ETH), and jasmonic acid (JA) regulate the formation of lily bulbs. We filtered a large number of DEGs involved in phytohormone synthesis and the signal transduction pathway from all pairwise comparisons to analyze their effects on the development of lily stem bulblets.

In this study, we hypothesized that genes related to cytokinin biosynthesis and signaling would undergo larger changes in expression levels compared to the control groups due to the application of 6-BA. We identified one *IPT3* (Isoform0002852) gene encoding isopentenyl transferase, which expression is up-regulated at B1 and down-regulated at the B10 and B20 stages. In contrast, most of the genes related to cytokinin degradation (*CKXs*) were down-regulated in expression at B1, but showed an up-regulated expression pattern at B10, including *CKX3* (Isoform0002852), *CKX5* (Isoform0002852), *CKX8* (Isoform0002852), *CKX9* (Isoform0002852), and *CKX11* (Isoform0002852) (Table S4). We also identified genes related to cytokinin signaling, such as cytokinin receptors (*AHKs*), phosphotransmitters (*AHPs*), and cytokinin response regulators (*RRs*). Among them, the *AHK3* gene was down-regulated at B1 and up-regulated at B10 and B20 stages. However, the *AHP4* gene was induced to be up-regulated by CK at B1 and down-regulated in expression at the following two periods (B10 and B20) as compared to control groups. Meanwhile, the response regulator *ARR12* (Isoform0019327) was significantly upregulated in 6-BA treated groups (Figure 4a).

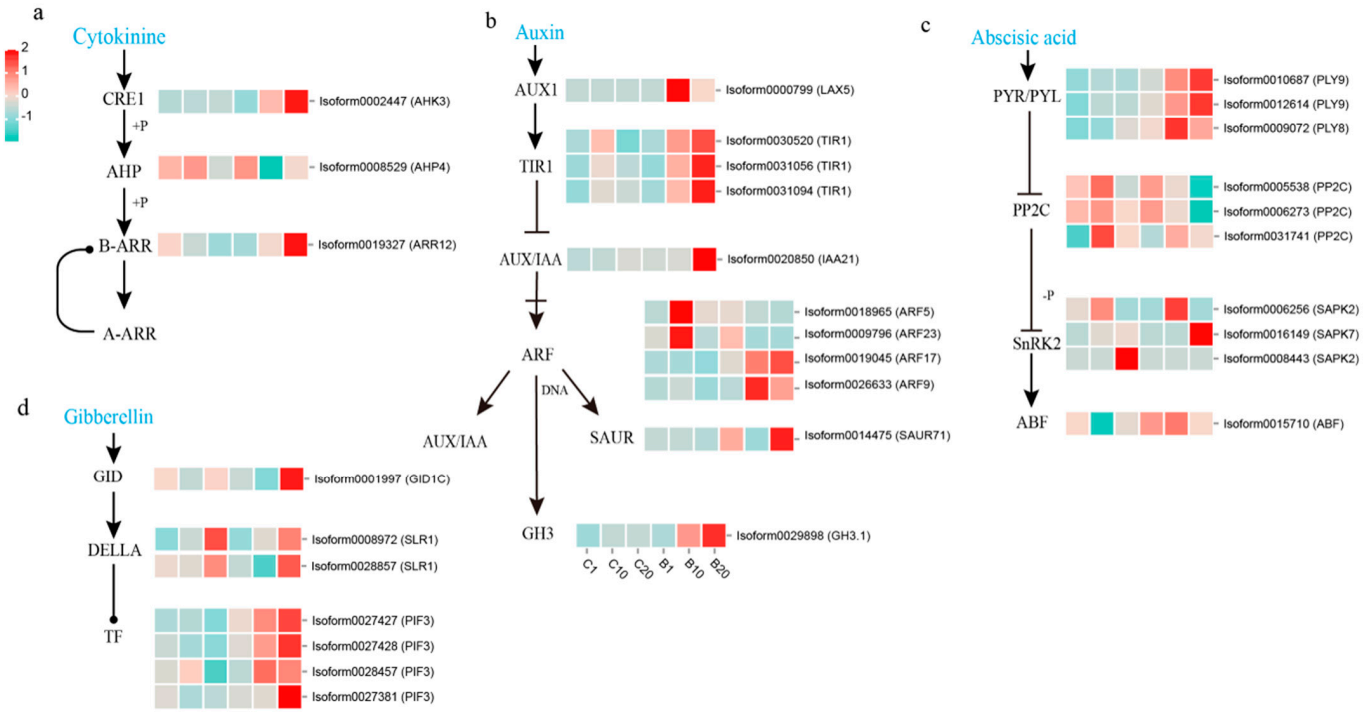

Figure 4. (**a**–**d**) Heatmap of the expression of DEGs related to plant hormone signal transduction pathway in the indicated groups during bulblet initiation, respectively. The gene expression levels are standardized into Z−scores, with red indicating upregulation and blue indicating downregulation.

In the auxin signaling pathway, the expression of the auxin transporter-like protein (*LAX5*) (Isoform0000799) increased in response to the 6-BA treatment after 10 and 20 days (Table S4). Similarly, we identified an auxin efflux carrier, *PIN1* (Isoform0012372), which was expressed at higher levels at B10 and B20 (Table S4). The transport inhibitor response 1 genes (*TIR1s*) did not show significant changes in gene expression at B1 and B10, but exhibited up-regulation at B20 vs. C20. In our study, the indole-3-acetic acid inducible gene (*IAA21*) was up-regulated at B20. We observed that several auxin response factor genes were induced by 6-BA, including *ARF5*, *ARF9*, *ARF17*, and *ARF23*. Among them, *ARF5* (Isoform0018965) and *ARF23* (Isoform0009796) exhibited an up-regulation pattern at B1. Meanwhile, the expression of *ARF17* (Isoform0019045) and *ARF9* (Isoform0026633) was significantly higher at 10 and 20 days in samples treated with 6-BA. In addition, the small auxin upregulated RNA gene (*SAUR71*) (Isoform0014475) was also upregulated in response to 6-BA after 20 days. At B10 and B20, there was an upregulation of the *GH3* gene (Isoform0029898), which encodes the enzyme IAA-amido synthetase, responsible for converting IAA to amino acids (Figure 4b).

In the ABA signaling pathway, abscisic acid receptor *PYL* genes (Isoform0010687, Isoform0012614 and Isoform0009072) were upregulated at B10 and B20. In contrast, two genes encoding *PP2C* (Isoform0005538 and Isoform0006273), a negative regulator of ABA, had a down-regulation at B20. The expression of serine/threonine-protein kinase (*SAPK*) genes, which contribute to ABA signaling, was mostly down-regulated (Figure 4c). As for GA metabolism, two *GA2OX* genes encoding GA2-beta-dioxygenase showed a downregulation at B10 and B20 (Table S4). Moreover, in the GA signal pathway, one GA receptor *GID1C* (Isoform001997) and one *SLR* gene (Isoform0028857) encoding DELLA protein were downregulated at B10 compared to C10. In contrast, one *SLR* gene (Isoform0008972) and four GA-regulated transcription factors *PIF3* (Isoform0027427, Isoform0027428 and Isoform0028457) showed different degrees of up-regulation in the three periods after 6-BA application (Figure 4d).

Additionally, numerous genes were related to brassinosteroid, ethylene, and jasmonic acid pathways. As for BR signaling, five *CYP* genes involved in BR biosynthesis were signif-

icantly upregulated in B10 and B20 compared to C10 and C20. Consistent herewith, *CURL3* (brassinosteroid insensitive 1 protein) and *BSK3* (brassinosteroid insensitive 2 protein) were upregulated during three periods under the 6-BA treatment. The 6-BA stress also led to up-regulation of several *XTH* genes encoding xyloglucan endotransglucosylase/hydrolase proteins. The ethylene signaling transduction pathway contains eight genes, among which three ethylene insensitive 3 (*EIN3*) genes and two *EBF1* genes encoding EIN3-binding F-box protein were downregulated at B10, while ethylene receptor (*ETR3*) was upregulated at B10. In terms of JA, three JAZ genes, which encode a protein with a ZIM domain, were primarily downregulated over the course of three treated periods. However, except for one *JAZ* gene (Isoform0016877), which was significantly upregulated by 6.04-fold at B10 vs. C10. Meanwhile, jasmonic acid-amino synthetase (*GH3.5*) and coronatine-insensitive protein 1 (*COI1*) were identified (Table S4).

3.6. Co-Expression Network Construction and Identification of WGCNA Modules

WGCNA allows clustering genes with similar expression patterns and analyzing the association between modules and specific traits or phenotypes. Based on the resemblance of expression profiles in our investigation, 16 modules were found (Figure S5a). Genes in the modules were evaluated using cluster analysis, which is shown using a heat map (Figure S5b). Furthermore, correlations between modules and samples were established to discern modules that exhibited significant associations with different treatments and stages (Figure S5c). Black module was significantly correlated with sample B1 (0.91), ivory module was strongly correlated with C10 (0.81), darkgreen module was positively correlated with samples B10 and B20 (0.47 and 0.66), and darkgreenolive2 module was most strongly correlated with C20 (0.89).

To identify the core modules, the expression profiles of the four obtained modules may be evaluated, as the eigengene expression patterns describe the changes in gene expression for the whole module. We found that eigengenes in the black module were up-regulated at B1 and down-regulated in all other samples (Figure S5d). Furthermore, the eigengene expression of the ivory module was down-regulated at all three periods under 6-BA treatment, but the eigengenes were significantly up-regulated at both C10 and C20 (Figure S5e). The eigengenes in the darkgreen module showed up-regulated expression at the B10 and B20 periods, while the genes in the control group showed a down-regulated pattern at all three periods (Figure S5f). The eigengenes of darkgreenolive2 module were also highly expressed only in C20. Subsequently, we annotated the four modules by KEGG analysis. According to the enrichment of KEGG, there were only three pathways in the black module with $p < 0.05$, which were "linoleic acid metabolism", "proteasome" and "peroxisome". The ivory module was clustered to two pathways regulated to hormone biosynthesis and signaling transduction (Figure S6). Similarly, the darkgreen module was enriched for three pathways related to phytohormones, which are "plant hormone signal transduction", "brassinosteroid biosynthesis" and "zeatin biosynthesis". Meanwhile, the darkgreenolive2 module genes were significantly enriched in the "starch and sucrose metabolism" pathway (Figure S6). It has been shown that the genes related to lily bulblet development are mainly enriched in two KEGG pathways, the plant hormone metabolism and the starch and sucrose pathways, respectively [3,18,19,37,38]. Therefore, the initial response of lily bulbs to 6-BA treatment may be strongly affected by the darkgreen, ivory and darkgreenolive2 module genes, so we focused on the in-depth analysis of the gene regulatory relationships of these three modules.

3.7. Identification of Hub TFs and Network Construction

To elucidate the regulatory role played by transcription factors on the formation of stem bulblets, we constructed network relationships between transcription factors in each module and genes significantly enriched in the hormone signaling transduction and starch and sucrose metabolism pathways We analyzed the DEGs of each module and screened the TFs with high connectivity in the network relationships as hub genes. According to

previous studies, the regulation of TFs such as HD-ZIP, TALE, MYB, BHLH, and others plays a pivotal role in the formation of new organs in plants [39].

In the darkgreen module, we found seven highly connected transcription factors as hub genes, which are HOX20 (Isoform0008631), AP2 (Isoform0002884), BLH4 (Isoform 0002562), LRP1 (Isoform0004786), ARR1 (Isoform0027655), and ARR12 (Isoform0000808). Through the gene expression heatmap, we found that except for BLH4 whose expression was down-regulated in B10 and B20 compared to the control group, the rest of the hub TFs expressed were up-regulated (Figure 5a). In the ivory module, we found many ERFs, SBPs, WRKYs, MYBs, and TALEs were identified as hub TFs. Among them, WRKYs and ERFs were the two most abundant TFs, with 15 and 10, respectively. Interestingly, BLH9 and the two SPL15 TFs expressed extremely high rates of crosstalk, and we found that all three genes were significantly down-regulated after 10 days of treatment by gene expression analysis (Figure 5b). Based on the gene connectivity relationships in the darkolivegreen2 module, a large number of TFs were found to be enriched in the module, among which were MYBs, GRAs, TALEs, and BHLHs. In addition, the two genes encoding ARF5 and HOX32 showed a high degree of connectivity in darkolivegreen2, and the expression of HOX32 was greater than that of C10 during the B10 period, whereas the expression of ARF5 was greater than that of C20 at the B20 stage (Figure 5c). From the above analysis, we know that the formation of stem bulblets is inextricably related to the collaborative regulation of multiple transcription factors.

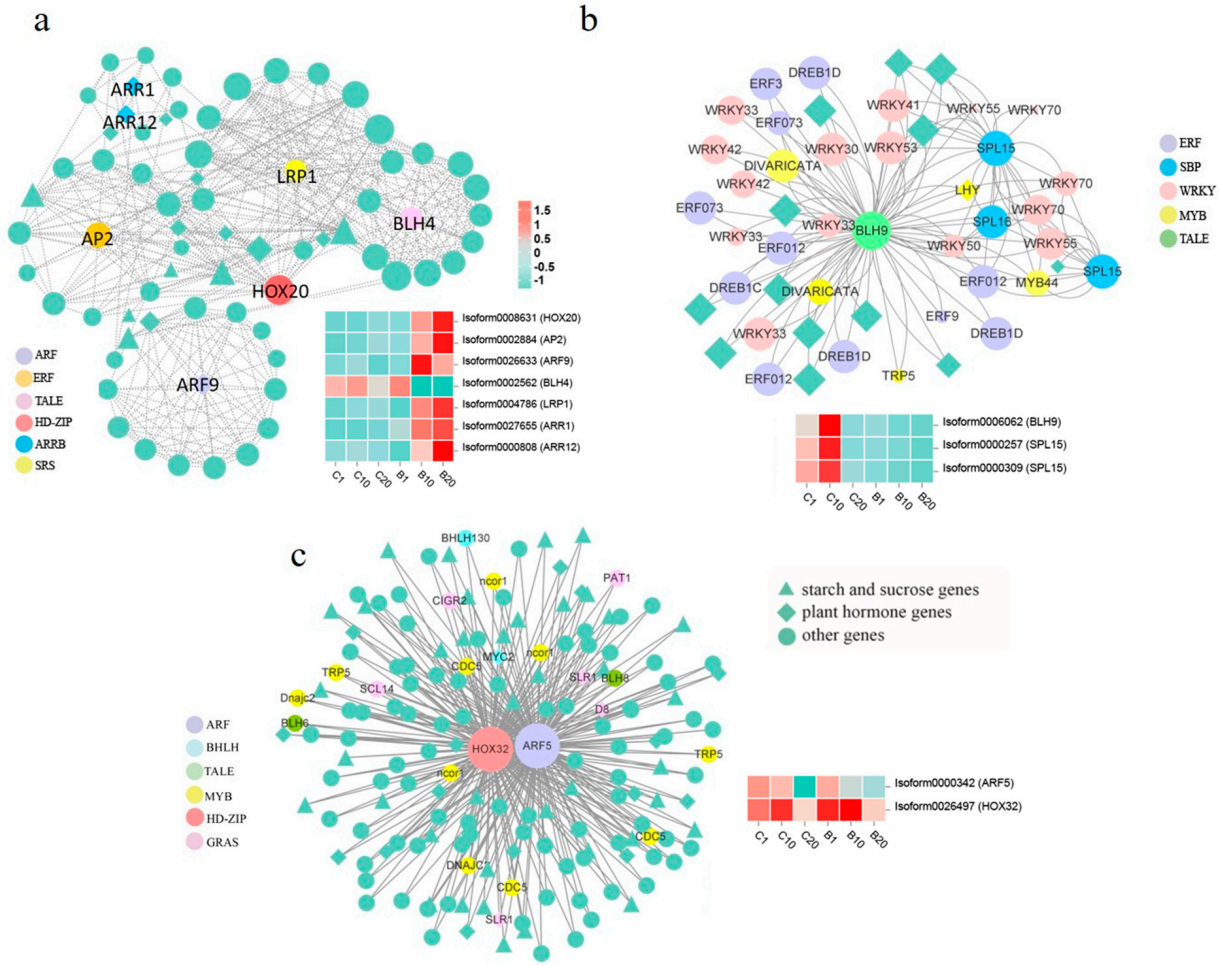

Figure 5. Identification and selection of vital transcription factors in four modules. (**a**) Network analysis of TFs in darkgreen module. (**b**) Network of the related genes in ivory module. (**c**) Network analysis of hub TFs in darkolivegreen2 module. The gene expression levels are standardized into Z−scores, with red indicating upregulation and green indicating downregulation.

4. Discussion

4.1. The Starch and Sucrose Metabolism Mediates Lily Stem Bulblet Initiation

As shown by the KEGG enrichment data, a significant portion of the genes in our study were enriched for the starch and sucrose metabolic pathways, demonstrating that carbohydrate metabolism affected bulblet formation in response to CK signaling under the application of 6-BA. Vacuolar convertase (INV) and sucrose synthase (SUS) are key components of the response to CK [40]. In lilies, previous studies demonstrated that high expression of *SUSs* may induce bulblet initiation in scales or leaf axils [3,16,18,19,41,42]. In our study, all six *SUS1* genes were up-regulated at B10 vs. C10, suggesting that *SUS1* can positively regulate bulblet formation and that the period of 10 days after 6-BA application may be the critical time point for bulblet initiation. In *Lycoris*, the expression of *INVs* was dramatically up-regulated to promote bulbogenesis, while leading to a decrease in sucrose content in maternal scales [43]. Similarly, the invertase (INV) activity in leaf axils was significantly increased, leading to the fact that sucrose can exert its signaling function by rapidly breaking down hexose to promote bulbil formation [42]. Here, the expression levels of *INVs* were significantly increased by 6-BA, showing a possible role of *INVs* in increasing bulblet regeneration ability.

The synthesis of starch is widely recognized as a pivotal process in the initiation of bulblets. Many investigations have suggested that the ability of a meristem to generate bublet primordia is contingent upon its aptitude to amass starch [44]. In *L. radiata*, AGPase as a major starch synthase was shown to be relevant in bulb expansion [43]. In this study, the *AGPS1* genes encoding AGPase exhibited an upregulated expression pattern in B10 vs. C10. Trehalose 6-phosphate (Tre6P) is an intermediate in trehalose biosynthesis, and it has been suggested that Tre6P can act as a signal for sugar supply that may be specific to the sucrose state [45]. Enhanced sucrose signaling during yam bulbil initiation leads to upregulation of TPS genes as well as downregulation of TPP genes. These up-regulated TPS genes can increase T6P levels, which can promote bulbil growth [46]. In our study, most of the *TPS* genes were up-regulated in 6-BA-treated groups compared to the control groups, especially at the time of 20 days of treatment. So, it may be speculated that genes related to sucrose synthesis such as *SUSs* and *INVs* were triggered to be up-regulated at B10 and thus positively affected *TPS* expression. All these results suggest that 6-BA as a CK signal can influence the metabolism of starch and sucrose and thus play a key positive regulatory role in the initiation of lily stem bulblets.

4.2. The Involvement of 6-BA in Plant Hormone Signal Transduction in Stem Bulblet Formation

In lily, CK was found to stimulate the outgrowth of bulblets or bulbils when directly applied to the scale or axillary part of the stem [9,10,47]. However, transcriptome analysis related to lily bulbogenesis after 6-BA is currently imposed. In transcriptome analyses of axillary bud formation in apple, samples treated with 6-BA show differences in the expression of genes related to CK synthesis and signal transduction. Among them, the expression of *IPT* genes related to cytokinin synthesis as well as CK degradation gene *CKXs* were highly expressed after 6-BA treatment [48]. In the present study, the expression of *IPT3* and several *CKXs* increased at B1 and B10, respectively. Furthermore, the upregulation of the cytokinin receptor gene *AHK*3 on B10 and B20 is observed. In the case of *L. lancifolium*, the application of 6-BA on scales also enhances the expression of the *AHKs* gene, which is consistent with our experimental results and further validates the reliability of our data. In *L. lancifolium*, the level of type-B *LlRR*s expression was found to be more pronounced in the axillary meristematic (AM) tissue compared to other tissues in lilies. It was also verified by the VIGs experiment that silencing *LlRR*s decreases the induction rate of bulbils. Moreover, *LlRR*s could bind to the promoters of *LlWOX9* and *LlWOX11* and promote their transcription to regulate the bulbil formation [26]. In this study, the B-type *ARR* gene (*ARR12*) was up-regulated in expression at all 6-BA samples. Taken as a whole, we conclude that CK signaling encourages cell proliferation and is crucial for bulb formation.

Research conducted on *L. lancifolium* revealed that the phenomenon of bulb formation in this particular plant serves as a noteworthy illustration of axillary organogenesis [10]. Simultaneously, auxins play a substantial role in fostering the growth of axillary meristematic tissue cells and the initiation of lateral organs [49]. In *yam*, high expression of auxin transporter proteins, including PINs and LAXs, triggered bulbil growth [46]. Research conducted on *Agave tequilana* has demonstrated that the upregulation of *AtqSoPIN1* expression can be triggered by the elimination of flower buds, resulting in the accumulation of auxin [50]. Consequently, this process stimulates the formation of bulbils. In our investigation, it was observed that the genes *PIN1* and *LAX5* exhibited a significant increase in expression levels at 10 and 20 days subsequent to the application of 6-BA. This observation leads to the proposition that the augmented expression of these genes, which are related to the transport of auxin, might play a crucial role in facilitating the process of lily stem bulblet formation. In our study, it was discovered that the four *ARF* genes displayed distinct patterns of expression at various stages following the induction by 6-BA. Specifically, *ARF5* and *ARF23* exhibited an increase in expression levels at B10, whereas *ARF17* and *ARF9* demonstrated an up-regulation at both B10 and B20. Genes related to the auxin signaling were significantly up-regulated in the sample group after treatment with 2,4-D, especially *ARFs*, which were expressed in an up-regulated pattern in the treated group, similar to our findings [16]. Therefore, we concluded that both 6-BA and 2,4-D could promote auxin signaling transduction.

In the current study, 6-BA administration upregulated *PYL* expression while down-regulating *PP2C* and *SAPK7* expression. As a result, 6-BA administration increased the expression of downstream genes involved in ABA anabolism, which prevented the growth of bulbs. In a prior study, the same findings showed that ABA had an inhibiting influence on bulb growth [43]. Our transcriptome results demonstrated that most BR and JA signaling pathway-related genes were expressed at higher levels in the 6-BA-treated group compared to the control group. In *P. ternate*, BR application can increase the content of GA and BR in bulbils, and decreased the ABA content [51]. A previous study showed that JA regulates tulip bulbs, and ectopic overexpression of *TgLOX4* and *TgLOX5* in Arabidopsis raised endogenous JA levels, promoted plant development, and multiplied the number of lateral roots [52]. Overall, we hypothesize that BR and JA can positively regulate the formation of bulbs. In addition, 6-BA treatment up-regulated *ETR* and down-regulated *EIN* and *EBF* in the ethylene signaling pathway. Together, 6-BA treatment may control the shift in plant hormone signal transduction to promote the production of stem bulblets.

4.3. TFs Involved in Bulblet Formation

In this study, the WGCNA and transcriptional regulatory modules were analyzed to screen out the highly connected transcription factors in the modules, and specific analysis was performed on the hub genes.

The TALE superfamily of genes is ubiquitous in plants and is involved in meristem development, leaf structure, and tuber formation [53]. It includes two subfamily members, KNOTTED1-like homeobox (KNOX) and BEL1-like homeobox (BELL or BLH) [54]. In the model plant Arabidopsis (*A. thaliana*), the BEL1 transcription factor regulates the production of lateral progenitors during ovule development and maintenance of the undifferentiated state of the inflorescence meristem by interacting with SHOOT MERISTEMLESS (STM) [55,56]. PENNYWISE(PNY)/BLH9 and POUND-FOOLISH(PNF)/BLH8 transcription factors promote normal meristematic structure both by interacting with BREVIPEDICELLU(BP)/KNAT1 and STM transcription factors in the class I KNOX subfamily [57–59]. In addition, BLH6 can negatively regulate the expression of secondary cell wall-related genes, and the secondary cell wall of the mutant *blh6* is thicker than that of the wild type [60]. In our study, all three modules were enriched for TALE family transcription factors, and BLH4 and BLH9 showed high connectivity in the darkgreen and ivory modules, respectively (Figure 5a,b). These two genes showed genetically down-regulated expression

at the critical stages of bulb initiation and formation, i.e., B10 and B20, and, therefore, we hypothesized that they may exercise a negative regulatory role in bulblet development.

The APETALA2/Ethylene Responsive Factor (AP2/ERF) transcription factors have been shown to integrate multiple stress-related hormones during development to activate cell division and lead to organogenesis [61]. In *Lilium*, it was found that external wounding first activates LoERF109, which is closely related to the auxin metabolic pathway, and *LoERF115*, which confers the ability to divide cells during organ regeneration *LoERF115* [62–64]. According to a study, EBE has an impact on Arabidopsis cell proliferation, axillary bud outgrowth, and shoot branching [65]. The *AP2* gene in the darkgreen module maintains high expression at the B10 versus B20 stage and may promote bulb formation (Figure 5a).

An earlier investigation found that the transcription factor AUXIN RESPONSE FACTOR 5 (ARF5) facilitated the initiation of auxin-dependent organs [49]. In old leaf axils of Arabidopsis, *AtARF5* up-regulates the expression of *ARGONAUTE10* (*AtAGO10*) [66], which can regulate the expression of HD-ZIP III as a target by competing with *AtAGO1* and specifically binding to miR166/165, to regulate AM [67]. HD-Zip transcription factors participate in plant organ and vascular development, meristem maintenance, regulation of hormones, and participation in responses to environmental conditions [68]. Among them, PHABULOSA (PHB), PHAVOLUTA (PHV), and REVOLUT (REV) belong to the HD-ZIP III subfamily, which have overlapping roles in embryogenesis and leaf polarity determination and are involved in the establishment of root tip bilateral symmetry and shoot apical meristem [69]. In the analysis, the HOX32 transcription factor in darkolivegreen2 module shared the same structural domain as the transcription factor of HD-Zip III. At the same time, we were surprised to find that HOX32 and ARF5 showed extremely high connectivity in the module, with which we boldly predicted that the interaction between these two genes might be important for bulblet formation, but the exact function needs further experimental validation (Figure 5c).

SQUAMOSA PROMOTER BINDING PROTEIN LIKE (SPL) controls many aspects of plant development and physiology, including the vegetative phase change, flowering time, leaf initiation, shoot and inflorescence branching [70]. In a previous study, miRNA156 could promote shoot branching and the vegetative to reproductive phase transition by regulating SPL9 and SPL15 [71]. In *lilium*, *LbrSPL9* and *LbrSPL15* could regulate phase transition [72]. In the ivory module, genes encoding SPL15 demonstrated extreme connectivity and we speculated that the initiation of bulbs may be facilitated (Figure 5b). Through WGCNA analysis, we similarly screened for MYBs, WRKYs, NACs, GRAs, BHLHs, ARRs, and other transcription factors, suggesting that the regulation of bulblet initiation is subject to the synergistic cooperation of multiple transcription factors and that the specific functions require further analysis.

5. Conclusions

The information gathered in this study provides a fresh perspective for a comprehensive understanding of the molecular processes, revealing the molecular mechanisms through which 6-BA promotes the formation of lily stem bulblets. Based on morphological and histological analyses, we divided the stimulation of underground stem bulblets by 6-BA into three stages: (1) axillary meristem activation stage (B1–B10), (2) bulblet initiation stage (axillary meristem formation stage) (B20), and (3) bulblet primordia formation stage (B25). Transcriptome sequencing was performed on leaf axil samples during the first two stages, covering three time points (1, 10, 20 days). Through the enrichment of KEGG pathways based on differentially expressed genes in various comparison groups, it was observed that 6-BA treatment had a significant impact on "plant hormone transduction" and "carbohydrate metabolism" pathways. Therefore, we propose a schematic model based on our findings (Figure 6). The *SUS1* gene, which is involved in sucrose synthesis, was up-regulated at the critical stage, so we hypothesized that sucrose may act as a signal to promote bulb growth by up-regulating a gene involved in the T6P pathway (*TPS6*). In addition, auxin is consumed and transported through up-regulation of auxin conjugated

gene (*GH3.1*) and auxin efflux proteins (*PIN1* and *LAX5*) to maintain bulb growth. *ARF9*, a gene related to growth hormone signaling, was up-regulated in expression relative to the control groups during the bulb initiation and formation period (B10 and B20). CK promotes its growth by rapidly activating the CK receptor (*AHK3*) gene while raising the cytokinin type-B response regulators (*ARR12*). By WGCNA analysis, we obtained the core transcription factors. It is possible that TFs such as BLHs, ARFs, HD-ZIPs, AP2/ERFs, and SBPs play a role in mediating cytokinin signaling and promoting stem bulblet formation.

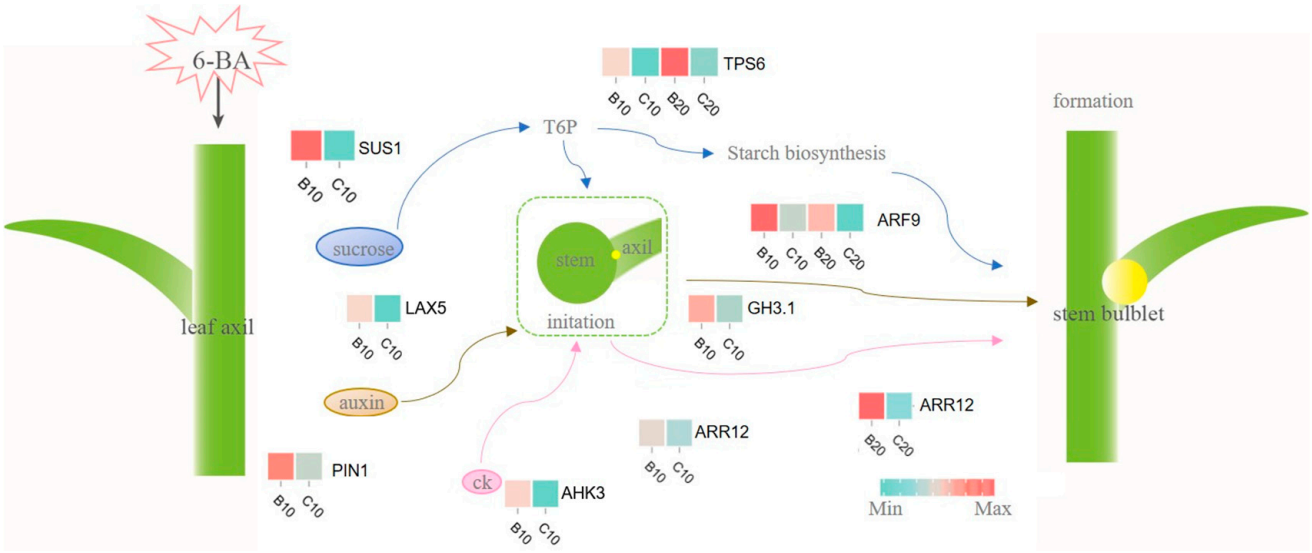

Figure 6. Schematic modeling of gene regulation by auxin, cytokinin, and sucrose during bulblet initiation and formation. The gene expression levels are standardized into Z-scores, with red indicating upregulation and green indicating downregulation.

In this study, after 6-BA treatment, genes involved in the synthesis and signal transduction of different phytohormones and starch and sucrose metabolism were differentially expressed, forming a comprehensive regulatory network to promote bulb formation. To establish the groundwork for the cultivation of lily cultivars with notable rejuvenation rates, it is imperative to prioritize additional investigations concerning the functional authentication of pivotal TFs. Furthermore, a more comprehensive exploration of the precise mechanisms underlying bulb development is warranted.

Supplementary Materials: The following supporting information can be downloaded at: https://www.mdpi.com/article/10.3390/horticulturae10020171/s1. Figure S1: Morphology and anatomy of control samples. Figure S2: Induction rate of the control group and 6-BA treated group during in stem bulblet initiation. Figure S3: PacBio Iso-Seq and expression profiles of *L.* 'Aladdin'. Figure S4: Expression of representative genes determined by RNA-seq and qRT-PCR. Figure S5: WGCNA network of axil samples. Figure S6: Top 20 KEGG pathways in each relevant module. Table S1: The primer sequences required for qRT-PCR. Table S2: Statistical summary of the reference transcriptome. Table S3: Starch and sucrose metabolism-related genes that were differentially expressed in response to 6-BA treatment. Table S4: Differently-expressed related to hormone metabolism and signaling in response to 6-BA treatment.

Author Contributions: K.Z., T.L. and Y.L. conceptualized and designed the experiment; K.Z. and T.L. performed the laboratory experiments and statical analysis; K.Z. and T.L. wrote and revised the manuscript; Y.L. funding acquisition and supervision. All authors have read and agreed to the published version of the manuscript.

Funding: This work was supported by the National Key R&D Program of China (grant No. 2019YFD1000400) and the China National Natural Science Foundation (grant No. 31872138).

Institutional Review Board Statement: Not applicable.

Informed Consent Statement: Not applicable.

Data Availability Statement: Data are contained within the article and Supplementary Materials.

Conflicts of Interest: The authors declare no conflict of interest.

References

1. Nhut, D.T. Micropropagation of lily (*Lilium longiflorum*) via in vitro stem node and pseudo-bulblet culture. *Plant Cell Rep.* **1998**, *17*, 913–916. [CrossRef]
2. Zhang, Y.; Yong, Y.B.; Wang, Q.; Lu, Y.M. Physiological and Molecular Changes during Lily Underground Stem Axillary Bulbils Formation. *Russ. J. Plant Physiol.* **2018**, *65*, 372–383. [CrossRef]
3. Yang, P.; Xu, L.; Xu, H.; Tang, Y.; He, G.; Cao, Y.; Feng, Y.; Yuan, S.; Ming, J. Histological and Transcriptomic Analysis during Bulbil Formation in *Lilium lancifolium*. *Front. Plant Sci.* **2017**, *8*, 1508. [CrossRef] [PubMed]
4. Moreno-Pachón, N. Mechanisms of Vegetative Propagation in Bulbs: A Molecular Approach. Ph.D. Dissertation, Wageningen University, Wageningen, The Netherlands, 2017.
5. Chatfield, S.P.; Raizada, M.N. Ethylene and shoot regeneration: Hookless1 modulates de novo shoot organogenesis in *Arabidopsis thaliana*. *Plant Cell Rep.* **2008**, *27*, 655–666. [CrossRef] [PubMed]
6. Motte, H.; Vereecke, D.; Geelen, D.; Werbrouck, S. The molecular path to in vitro shoot regeneration. *Biotechnol. Adv.* **2014**, *32*, 107–121. [CrossRef]
7. Sang, Y.L.; Cheng, Z.J.; Zhang, X.S. Plant stem cells and de novo organogenesis. *New Phytol.* **2018**, *218*, 1334–1339. [CrossRef]
8. Greb, T.; Clarenz, O.; Schafer, E.; Muller, D.; Herrero, R.; Schmitz, G.; Theres, K. Molecular analysis of the LATERAL SUPPRESSOR gene in *Arabidopsis* reveals a conserved control mechanism for axillary meristem formation. *Genes. Dev.* **2003**, *17*, 1175–1187. [CrossRef]
9. Zhang, Y.; Zeng, Z.; Yong, Y.B.; Lyu, Y.M. Hormonal Regulatory Patterns of LaKNOXs and LaBEL1 Transcription Factors Reveal Their Potential Role in Stem Bulblet Formation in LA Hybrid Lily. *Int. J. Mol. Sci.* **2021**, *22*, 13502. [CrossRef]
10. He, G.; Yang, P.; Tang, Y.; Cao, Y.; Qi, X.; Xu, L.; Ming, J. Mechanism of exogenous cytokinins inducing bulbil formation in *Lilium lancifolium* in vitro. *Plant Cell Rep.* **2020**, *39*, 861–872. [CrossRef]
11. Rosspopoff, O.; Chelysheva, L.; Saffar, J.; Lecorgne, L.; Gey, D.; Caillieux, E.; Colot, V.; Roudier, F.; Hilson, P.; Berthomé, R.; et al. Direct conversion of root primordium into shoot meristem relies on timing of stem cell niche development. *Development* **2017**, *144*, 1187–1200. [CrossRef]
12. de Reuille, P.B.; Bohn-Courseau, I.; Ljung, K.; Morin, H.; Carraro, N.; Godin, C.; Traas, J. Computer simulations reveal properties of the cell-cell signaling network at the shoot apex in *Arabidopsis*. *Proc. Natl. Acad. Sci. USA* **2006**, *103*, 1627–1632. [CrossRef] [PubMed]
13. Heisler, M.G.; Ohno, C.; Das, P.; Sieber, P.; Reddy, G.V.; Long, J.A.; Meyerowitz, E.M. Patterns of auxin transport and gene expression during primordium development revealed by live imaging of the *Arabidopsis* inflorescence meristem. *Curr. Biol.* **2005**, *15*, 1899–1911. [CrossRef] [PubMed]
14. Tang, Y. *The Mechanism of Auxin Involving in Bulbil Formation of Lilium lancifolium*; Chinese Academy of Agricultural Sciences: Beijing, China, 2019.
15. Li, J.; Sun, M.; Li, H.; Ling, Z.; Wang, D.; Zhang, J.; Shi, L. Full-length transcriptome-referenced analysis reveals crucial roles of hormone and wounding during induction of aerial bulbils in lily. *BMC Plant Biol.* **2022**, *22*, 415. [CrossRef]
16. Gao, C.; Zhang, L.; Xu, Y.; Liu, Y.; Xiao, X.; Cui, L.; Xia, Y.; Wu, Y.; Ren, Z. Full-length transcriptome analysis revealed that 2,4-dichlorophenoxyacetic acid promoted in vitro bulblet initiation in lily by affecting carbohydrate metabolism and auxin signaling. *Front. Plant Sci.* **2023**, *14*, 1236315. [CrossRef]
17. Gao, M.; Zhang, S.; Luo, C.; He, X.; Wei, S.; Jiang, W.; He, F.; Lin, Z.; Yan, M.; Dong, W. Transcriptome analysis of starch and sucrose metabolism across bulb development in *Sagittaria sagittifolia*. *Gene* **2018**, *649*, 99–112. [CrossRef]
18. Li, X.Y.; Wang, C.X.; Cheng, J.Y.; Zhang, J.; da Silva, J.A.T.; Liu, X.Y.; Duan, X.; Li, T.L.; Sun, H.M. Transcriptome analysis of carbohydrate metabolism during bulblet formation and development in *Lilium davidii* var. *unicolor*. *BMC Plant Biol.* **2014**, *14*, 358. [CrossRef]
19. Wu, Y.; Ren, Z.; Gao, C.; Sun, M.; Li, S.; Min, R.; Wu, J.; Li, D.; Wang, X.; Wei, Y.; et al. Change in Sucrose Cleavage Pattern and Rapid Starch Accumulation Govern Lily Shoot-to-Bulblet Transition In Vitro. *Front. Plant Sci.* **2020**, *11*, 564713. [CrossRef]
20. Ren, Z.M.; Zhang, D.; Jiao, C.; Li, D.Q.; Wu, Y.; Wang, X.Y.; Gao, C.; Lin, Y.F.; Ruan, Y.L.; Xia, Y.P. Comparative transcriptome and metabolome analyses identified the mode of sucrose degradation as a metabolic marker for early vegetative propagation in bulbs of Lycoris. *Plant J.* **2022**, *112*, 115–134. [CrossRef]
21. Wang, Q.; Hasson, A.; Rossmann, S.; Theres, K. Divide et impera: Boundaries shape the plant body and initiate new meristems. *New Phytol.* **2016**, *209*, 485–498. [CrossRef] [PubMed]
22. Tian, C.; Zhang, X.; He, J.; Yu, H.; Wang, Y.; Shi, B.; Han, Y.; Wang, G.; Feng, X.; Zhang, C.; et al. An organ boundary-enriched gene regulatory network uncovers regulatory hierarchies underlying axillary meristem initiation. *Mol. Syst. Biol.* **2014**, *10*, 755. [CrossRef] [PubMed]
23. Yang, M.; Jiao, Y. Regulation of Axillary Meristem Initiation by Transcription Factors and Plant Hormones. *Front. Plant Sci.* **2016**, *7*, 183. [CrossRef] [PubMed]

24. Abraham-Juárez, M.J.; Martínez-Hernández, A.; Leyva-González, M.A.; Herrera-Estrella, L.; Simpson, J. Class I KNOX genes are associated with organogenesis during bulbil formation in Agave tequilana. *J. Exp. Bot.* **2010**, *61*, 4055–4067. [CrossRef] [PubMed]
25. Yang, P.; Xu, H.; Xu, L.; Tang, Y.; He, G.; Cao, Y.; Yuan, S.; Ren, J.; Ming, J. Cloning and expression analysis of LlAGO1 in *Lilium lancifolium*. *Acta Hortic. Sin.* **2018**, *45*, 784–794. [CrossRef]
26. He, G.; Cao, Y.; Wang, J.; Song, M.; Bi, M.; Tang, Y.; Xu, L.; Ming, J.; Yang, P. WUSCHEL-Related Homeobox Genes Cooperate with Cytokinin to Promote Bulbil Formation in *Lilium lancifolium*. *Plant Physiol.* **2022**, *190*, 387–402. [CrossRef] [PubMed]
27. Fang, S.; Yang, C.; Ali, M.M.; Lin, M.; Tian, S.; Zhang, L.; Chen, F.; Lin, Z. Transcriptome Analysis Reveals the Molecular Regularity Mechanism Underlying Stem Bulblet Formation in Oriental Lily 'Siberia'; Functional Characterization of the LoLOB18 Gene. *Int. J. Mol. Sci.* **2022**, *23*, 15246. [CrossRef] [PubMed]
28. Gordon, S.P.; Tseng, E.; Salamov, A.; Zhang, J.; Meng, X.; Zhao, Z.; Kang, D.; Underwood, J.; Grigoriev, I.V.; Figueroa, M.; et al. Widespread Polycistronic Transcripts in Fungi Revealed by Single-Molecule mRNA Sequencing. *PLoS ONE* **2015**, *10*, e0132628. [CrossRef] [PubMed]
29. Salmela, L.; Rivals, E. LoRDEC: Accurate and efficient long read error correction. *Bioinformatics* **2014**, *30*, 3506–3514. [CrossRef] [PubMed]
30. Li, R.; Yu, C.; Li, Y.; Lam, T.W.; Yiu, S.M.; Kristiansen, K.; Wang, J. SOAP2: An improved ultrafast tool for short read alignment. *Bioinformatics* **2009**, *25*, 1966–1967. [CrossRef]
31. Kim, D.; Langmead, B.; Salzberg, S.L. HISAT: A fast spliced aligner with low memory requirements. *Nat. Methods* **2015**, *12*, 357–360. [CrossRef]
32. Trapnell, C.; Williams, B.A.; Pertea, G.; Mortazavi, A.; Kwan, G.; van Baren, M.J.; Salzberg, S.L.; Wold, B.J.; Pachter, L. Transcript assembly and quantification by RNA-Seq reveals unannotated transcripts and isoform switching during cell differentiation. *Nat. Biotechnol.* **2010**, *28*, 511–515. [CrossRef]
33. Zhang, B.; Horvath, S. A general framework for weighted gene co-expression network analysis. *Stat. Appl. Genet. Mol. Biol.* **2005**, *4*, 17. [CrossRef]
34. Shannon, P.; Markiel, A.; Ozier, O.; Baliga, N.S.; Wang, J.T.; Ramage, D.; Amin, N.; Schwikowski, B.; Ideker, T. Cytoscape: A software environment for integrated models of biomolecular interaction networks. *Genome Res.* **2003**, *13*, 2498–2504. [CrossRef]
35. Livak, K.J.; Schmittgen, T.D. Analysis of relative gene expression data using real-time quantitative PCR and the 2(-Delta Delta C(T)) Method. *Methods* **2001**, *25*, 402–408. [CrossRef]
36. Liu, Q.; Wei, C.; Zhang, M.F.; Jia, G.X. Evaluation of putative reference genes for quantitative real-time PCR normalization in *Lilium regale* during development and under stress. *Peerj* **2016**, *4*, e1837. [CrossRef]
37. Qi, N.N.; Hou, X.M.; Wang, C.L.; Li, C.X.; Huang, D.J.; Li, Y.H.; Wang, N.; Liao, W.B.A. Methane-rich water induces bulblet formation of scale cuttings in *Lilium davidii* var. *unicolor* by regulating the signal transduction of phytohormones and their levels. *Physiol. Plant.* **2021**, *172*, 1919–1930. [CrossRef] [PubMed]
38. Hou, X.; Qi, N.; Wang, C.; Li, C.; Huang, D.; Li, Y.; Wang, N.; Liao, W. Hydrogen-rich water promotes the formation of bulblets in *Lilium davidii* var. *unicolor* through regulating sucrose and starch metabolism. *Planta* **2021**, *254*, 106. [CrossRef]
39. Schmitz, G.; Theres, K. Shoot and inflorescence branching. *Curr. Opin. Plant Biol.* **2005**, *8*, 506–511. [CrossRef] [PubMed]
40. Roman, H.; Girault, T.; Barbier, F.; Péron, T.; Brouard, N.; Pěnčík, A.; Novák, O.; Vian, A.; Sakr, S.; Lothier, J.; et al. Cytokinins Are Initial Targets of Light in the Control of Bud Outgrowth. *Plant Physiol.* **2016**, *172*, 489–509. [CrossRef] [PubMed]
41. Wang, F.; Sanz, A.; Brenner, M.L.; Smith, A. Sucrose Synthase, Starch Accumulation, and Tomato Fruit Sink Strength. *Plant Physiol.* **1993**, *101*, 321–327. [CrossRef] [PubMed]
42. Hao, C.; Yang, P.; Qu, Y.; Hao, Z.; Yin, X.; Tang, Y.; Bi, M.; Xu, L.; Hu, F.; Ming, J. Sucrose function on the bulbil formation of *Lilium lancifolium*. *Sci. Hortic.* **2024**, *323*, 112538. [CrossRef]
43. Xu, J.X.; Li, Q.Z.; Yang, L.Y.; Li, X.; Wang, Z.; Zhang, Y.C. Changes in carbohydrate metabolism and endogenous hormone regulation during bulblet initiation and development in *Lycoris radiata*. *BMC Plant Biol.* **2020**, *20*, 180. [CrossRef]
44. Wu, Y.; Sun, M.; Li, S.; Min, R.; Gao, C.; Lyu, Q.; Ren, Z.; Xia, Y. Molecular cloning, characterization and expression analysis of three key starch synthesis-related genes from the bulb of a rare lily germplasm, *Lilium brownii* var. *giganteum*. *J. Zhejiang Univ. Sci. B* **2021**, *22*, 476–491. [CrossRef]
45. Yadav, U.P.; Ivakov, A.; Feil, R.; Duan, G.Y.; Walther, D.; Giavalisco, P.; Piques, M.; Carillo, P.; Hubberten, H.M.; Stitt, M.; et al. The sucrose-trehalose 6-phosphate (Tre6P) nexus: Specificity and mechanisms of sucrose signalling by Tre6P. *J. Exp. Bot.* **2014**, *65*, 1051–1068. [CrossRef]
46. Wu, Z.G.; Jiang, W.; Tao, Z.M.; Pan, X.J.; Yu, W.H.; Huang, H.L. Morphological and stage-specific transcriptome analyses reveal distinct regulatory programs underlying yam (*Dioscorea alata* L.) bulbil growth. *J. Exp. Bot.* **2020**, *71*, 1899–1914. [CrossRef]
47. Mo, J.L.; Qu, Y.X.; He, G.R.; Yang, P.P.; Wang, L.H.; Zhang, L.N.; Wu, X.W.; Zhang, D.; Li, L.L.; Ming, J. Effect of exogenous 6-BA induced bulblets formation in aerial cultivation. *Sci. Hortic.* **2023**, *309*, 111644. [CrossRef]
48. Li, G.; Tan, M.; Cheng, F.; Liu, X.; Qi, S.; Chen, H.; Zhang, D.; Zhao, C.; Han, M.; Ma, J. Molecular role of cytokinin in bud activation and outgrowth in apple branching based on transcriptomic analysis. *Plant Mol. Biol.* **2018**, *98*, 261–274. [CrossRef]
49. Luo, L.; Zeng, J.; Wu, H.; Tian, Z.; Zhao, Z. A Molecular Framework for Auxin-Controlled Homeostasis of Shoot Stem Cells in *Arabidopsis*. *Mol. Plant* **2018**, *11*, 899–913. [CrossRef] [PubMed]

50. Abraham Juárez, M.J.; Hernández Cárdenas, R.; Santoyo Villa, J.N.; O'Connor, D.; Sluis, A.; Hake, S.; Ordaz-Ortiz, J.; Terry, L.; Simpson, J. Functionally different PIN proteins control auxin flux during bulbil development in *Agave tequilana*. *J. Exp. Bot.* **2015**, *66*, 3893–3905. [CrossRef] [PubMed]
51. Guo, C.; Li, J.; Li, M.; Xu, X.; Chen, Y.; Chu, J.; Yao, X. Regulation Mechanism of Exogenous Brassinolide on Bulbil Formation and Development in *Pinellia ternata*. *Front. Plant Sci.* **2021**, *12*, 809769. [CrossRef]
52. Ravnikar, M.; El, J.; Plaper, I.; Pacapan, A. Jasmonic acid stimulates shoot and bulb formation of garlic in vitro. *J. Plant Growth Regul.* **1993**, *12*, 73–77. [CrossRef]
53. Hamant, O.; Pautot, V. Plant development: A TALE story. *Comptes Rendus Biol.* **2010**, *333*, 371–381. [CrossRef]
54. Bürglin, T.R. Analysis of TALE superclass homeobox genes (MEIS, PBC, KNOX, Iroquois, TGIF) reveals a novel domain conserved between plants and animals. *Nucleic Acids Res.* **1997**, *25*, 4173–4180. [CrossRef]
55. Bellaoui, M.; Pidkowich, M.S.; Samach, A.; Kushalappa, K.; Kohalmi, S.E.; Modrusan, Z.; Crosby, W.L.; Haughn, G.W. The *Arabidopsis* BELL1 and KNOX TALE homeodomain proteins interact through a domain conserved between plants and animals. *Plant Cell* **2001**, *13*, 2455–2470. [CrossRef] [PubMed]
56. Robinson-Beers, K.; Pruitt, R.E.; Gasser, C.S. Ovule Development in Wild-Type *Arabidopsis* and Two Female-Sterile Mutants. *Plant Cell* **1992**, *4*, 1237–1249. [CrossRef] [PubMed]
57. Smith, H.M.; Hake, S. The interaction of two homeobox genes, BREVIPEDICELLUS and PENNYWISE, regulates internode patterning in the *Arabidopsis* inflorescence. *Plant Cell* **2003**, *15*, 1717–1727. [CrossRef]
58. Kanrar, S.; Onguka, O.; Smith, H.M. *Arabidopsis* inflorescence architecture requires the activities of KNOX-BELL homeodomain heterodimers. *Planta* **2006**, *224*, 1163–1173. [CrossRef] [PubMed]
59. Bhatt, A.M.; Etchells, J.P.; Canales, C.; Lagodienko, A.; Dickinson, H. VAAMANA—A BEL1-like homeodomain protein, interacts with KNOX proteins BP and STM and regulates inflorescence stem growth in *Arabidopsis*. *Gene* **2004**, *328*, 103–111. [CrossRef] [PubMed]
60. Liu, Y.; You, S.; Taylor-Teeples, M.; Li, W.L.; Schuetz, M.; Brady, S.M.; Douglas, C.J. BEL1-LIKE HOMEODOMAIN6 and KNOTTED *ARABIDOPSIS THALIANA7* interact and regulate secondary cell wall formation via repression of REVOLUTA. *Plant Cell* **2014**, *26*, 4843–4861. [CrossRef]
61. Licausi, F.; Ohme-Takagi, M.; Perata, P. APETALA2/Ethylene Responsive Factor (AP2/ERF) transcription factors: Mediators of stress responses and developmental programs. *New Phytol.* **2013**, *199*, 639–649. [CrossRef]
62. Mao, J.L.; Miao, Z.Q.; Wang, Z.; Yu, L.H.; Cai, X.T.; Xiang, C.B. *Arabidopsis* ERF1 Mediates Cross-Talk between Ethylene and Auxin Biosynthesis during Primary Root Elongation by Regulating ASA1 Expression. *PLoS Genet.* **2016**, *12*, e1005760. [CrossRef]
63. Cai, X.T.; Xu, P.; Zhao, P.X.; Liu, R.; Yu, L.H.; Xiang, C.B. *Arabidopsis* ERF109 mediates cross-talk between jasmonic acid and auxin biosynthesis during lateral root formation. *Nat. Commun.* **2014**, *5*, 5833. [CrossRef]
64. Heyman, J.; Cools, T.; Canher, B.; Shavialenka, S.; Traas, J.; Vercauteren, I.; Van den Daele, H.; Persiau, G.; De Jaeger, G.; Sugimoto, K.; et al. The heterodimeric transcription factor complex ERF115-PAT1 grants regeneration competence. *Nat. Plants* **2016**, *2*, 16165. [CrossRef]
65. Mehrnia, M.; Balazadeh, S.; Zanor, M.I.; Mueller-Roeber, B. EBE, an AP2/ERF transcription factor highly expressed in proliferating cells, affects shoot architecture in *Arabidopsis*. *Plant Physiol.* **2013**, *162*, 842–857. [CrossRef]
66. Zhang, C.; Fan, L.; Le, B.H.; Ye, P.; Mo, B.; Chen, X. Regulation of ARGONAUTE10 Expression Enables Temporal and Spatial Precision in Axillary Meristem Initiation in *Arabidopsis*. *Dev. Cell* **2020**, *55*, 603–616.e605. [CrossRef]
67. Zhu, H.L.; Hu, F.Q.; Wang, R.H.; Zhou, X.; Sze, S.H.; Liou, L.W.; Barefoot, A.; Dickman, M.; Zhang, X.R. *Arabidopsis* Argonaute10 Specifically Sequesters miR166/165 to Regulate Shoot Apical Meristem Development. *Cell* **2011**, *145*, 242–256. [CrossRef]
68. Ariel, F.D.; Manavella, P.A.; Dezar, C.A.; Chan, R.L. The true story of the HD-Zip family. *Trends Plant Sci.* **2007**, *12*, 419–426. [CrossRef] [PubMed]
69. Prigge, M.J.; Clark, S.E. Evolution of the class III HD-Zip gene family in land plants. *Evol. Dev.* **2006**, *8*, 350–361. [CrossRef] [PubMed]
70. Preston, J.C.; Hileman, L.C. Functional Evolution in the Plant SQUAMOSA-PROMOTER BINDING PROTEIN-LIKE (SPL) Gene Family. *Front. Plant Sci.* **2013**, *4*, 80. [CrossRef] [PubMed]
71. Schwarz, S.; Grande, A.V.; Bujdoso, N.; Saedler, H.; Huijser, P. The microRNA regulated SBP-box genes SPL9 and SPL15 control shoot maturation in *Arabidopsis*. *Plant Mol. Biol.* **2008**, *67*, 183–195. [CrossRef] [PubMed]
72. Zhao, M.; Liu, R.; Chen, Y.; Cui, J.; Ge, W.; Zhang, K. Molecular identification and functional verification of SPL9 and SPL15 of *Lilium*. *Mol. Genet. Genom.* **2022**, *297*, 63–74. [CrossRef] [PubMed]